Talanta 134 (2015) 699–704

Contents lists available at ScienceDirect

Talanta

journal homepage: www.elsevier.com/locate/talanta

A new electrochemical aptasensor based on electrocatalytic property of graphene toward ascorbic acid oxidation

Liang Wu [a,b], Erhu Xiong [a], Yue Yao [a], Xia Zhang [a], Xiaohua Zhang [a,*], Jinhua Chen [a,*]

[a] State Key Laboratory of Chemo/Biosensing and Chemometrics, College of Chemistry and Chemical Engineering, Hunan University, Changsha, 410082, P.R. China

[b] College of Chemistry and Life Science, Zhejiang Normal University, Jinhua 321004, China

ARTICLE INFO

Article history:
Received 15 August 2014
Received in revised form
8 December 2014
Accepted 11 December 2014
Available online 18 December 2014

Keywords:
Graphene
Nanocatalyst
Ascorbic acid
Adenosine triphosphate
Electrochemical aptasensor

ABSTRACT

Based on the superior electrocatalytic property of graphene (GN) toward ascorbic acid (AA) oxidation, a new electrochemical aptasensor has been developed. Here, adenosine triphosphate (ATP) is used as the model to demonstrate the performance of the developed aptasensor. Briefly, GN is attached to the thiolated ATP binding aptamer (ABA) modified gold electrode through π-π stacking interaction, resulting in a significant oxidation signal of AA. In the presence of ATP, the formation of ATP-ABA complex leads to the release of GN from sensing interface, resulting in a sharp decrease of the oxidation peak current of AA and an obviously positive shift of the related peak potential. Taking both the change values of the peak current and peak potential of AA oxidation as the response signals, ATP can be detected sensitively. This is the first time to demonstrate the application of GN as the nanocatalyst in an amplified aptasensor. It can be expected that GN, as nanocatalyst, should become the very promising amplifying-elements in DNA-based electrochemical biosensors.

1. Introduction

Graphene (GN) is a new form of carbon nanomaterials with single-atom-thick and two-dimensional structure [1]. Over the past years, GN and its related nanomaterials have been widely used in the DNA-based electrochemical sensors due to their good biological compatibility, high surface area and excellent electrochemical properties [2,3]. They are usually used as the electrode materials with good conductivity and abundant binding points [4–6], the carriers for loading numerous signal elements [7,8], the tracers based on their direct electrochemistry [9–11], and the mediators to regulate the electron transfer process [12]. For example, Akhavan et al. utilized the vertical reduced graphene nanowalls (RGNWs) as the porous electrode materials for an ultra-high-resolution electrochemical detection of the four bases of DNA [13]. Pumera et al. used graphene oxide nanoplatelets (GONPs) as the inherently electroactive tracers for DNA analysis [14]. Dong developed the impedimetric biosensors for the detection of ATP or Hg^{2+} based on the ultrahigh electron transfer ability of graphene [15]. Actually, GN and its related nanomaterials are also the preeminent nanocatalysts toward many substances, such as H_2O_2, ascorbic acid (AA), uric acid (UA) and dopamine (DA), etc [16,17]. In John's work, the electrochemically reduced graphene oxide (ERGO) showed the excellent electrocatalytic activity [18]. It not only enhanced the oxidation currents of AA, DA, and UA, but also shifted the oxidation potentials of them to less positive potentials compared to the bare glassy carbon electrode (GCE) and separated their electrochemical oxidation signals into three distinct peaks.

As we known, electrocatalysis represents a preferred means for signal amplification in electrochemical biosensors. Thanks to their superior electrocatalytic properties, many nanomaterials, especially the noble metal nanoparticles, have been widely employed as the signal amplification elements in DNA-based electrochemical biosensors [19–22]. Willner's group developed the amperometric biosensor for the amplified electrochemical detection of DNA and protein based on the Pt nanoparticles toward electrocatalytic reduction of H_2O_2 [23]. Cai et al. reported a new electrochemical strategy for the detection of hepatitis C virus using the electrocatalytic signal amplification method of Au nanoparticles combining with a conformation-switched hairpin DNA probe [24]. In general, nanocatalysts used in electrochemical sensors have many advantages, such as their high effective surface area offers a large number of active sites and often a high signal-to-noise ratio, their catalytic properties lead to a decrease in the overpotential needed for a reaction to become kinetically viable and their good conductivity causes a high rate of electron transport [25,26]. Moreover, nanocatalysts can also overcome the problems associated with the thermal and environmental instability inherent in biological materials (such as enzymes). Unfortunately, there is no report taking GN as the nanocatalyst for signal amplification in the

* Corresponding authors. Tel.: +86 731 88821848.
E-mail addresses: mickyxie@hnu.edu.cn (X. Zhang), chenjinhua@hnu.edu.cn (J. Chen).

http://dx.doi.org/10.1016/j.talanta.2014.12.011
0039-9140/

DNA-based electrochemical biosensors, although GN possesses excellent electrocatalytic property.

Aptamers are DNA or RNA molecules selected from random-sequence nucleic acid libraries using systematic evolution of ligands by exponential enrichment (SELEX). They have specific binding affinity to a variety of target molecules, such as drugs, organic or inorganic molecules, proteins, even cells [27]. Adenosine triphosphate (ATP) is generally acknowledged as the "energy currency" in most animate beings, which plays very important role in most enzymatic activities [28]. DNA-based ATP aptamer can bind two ATP molecules in a noncanonical, but stable, helix comprised of G:G and G:A base pairs flanked by short canonical helices [29].

In this paper, ATP and its aptamer were used as the model and a new electrochemical aptasensor has been developed based on the superior electrocatalytic property of GN to AA oxidation. As shown in Scheme 1, ATP binding aptamer (ABA) was firstly immobilized onto Au electrode via the Au-S bond (ABA/Au) [30,31]. Then, the aptamer could strongly adsorb GN due to the π-π interaction between GN and ABA (GN/ABA/Au) [32,33]. Because of the excellent catalytic property of GN, the obtained GN/ABA/Au electrode has showed a significantly electrocatalytic signal of AA oxidation. Upon the target binding, the formation of ATP-ABA complex led to the release of GN from the sensing interface, resulting in the decrease of the loading amount of nanocatalyst on the electrode. Such a conformational change not only results in the decrease of the oxidation peak current of AA, but also the positive shift of the related peak potential. Thus, sensitive detection of ATP can be realized by simultaneously monitoring the changes of the peak current (ΔI) and peak potential (ΔE) of AA. To our best knowledge, this is the first time to demonstrate the application of GN as the nanocatalyst in an amplified aptasensor. It can be expected that GN should become the very promising amplifying-elements in other DNA-based electrochemical biosensors.

2. Materials and methods

2.1. Reagents and materials

Graphene oxide (GO) was prepared from natural graphite powder through a modified Hummers method [34]. GN was prepared by chemical reduction of GO with hydrazine according to the literature [35]. Procedures were as follows: 240.0 μL of ammonia solution (25.0 wt %) and 14.5 μL of hydrazine hydrate (50.0 wt %) were added to 0.5 mg mL^{-1} GO (20.0 mL). After being vigorously stirred for a few minutes, the glass vial containing the above mixture was put in a water bath (95 °C) with continuously stirred for 1 h. Then, the product (GN) was centrifuged and washed with ultra pure water for several times, and dried in a vacuum oven at 60 °C for 48 h. Finally, a certain amount of GN was dispersed in ultra pure water with ultrasonication to prepare 0.5 mg mL^{-1} GN solution.

The ABA and another DNA strand which is not the ATP aptamer (NABA) were synthesized by Sangon Biotechnology Co. Ltd. (Shanghai, China). The sequence of ABA is 5'–SH-ACCTGGGGGAGTATTGCGGAG-GAAGGT-3' according to the literatures [15,36]. The sequence of NABA is 5'–SH-AGGAGCGCGAGAAGTGTGGTGCATGTG-3'. DNA stock solutions were prepared with Tris–HCl buffer (25.0 mM Tris–HCl, 150.0 mM NaCl, pH=7.4) and kept frozen. ATP, cytidine triphosphate (CTP), guanosine triphosphate (GTP) and uridine triphosphate (UTP) were obtained from Sangon Biotechnology Co. Ltd. (Shanghai, China). AA was purchased from Sinopharm Chemical Reagent Co. Ltd. (Shanghai, China). The AA solution (1.0 mM) was freshly prepared in phosphate buffer solutions (10.0 mM PBS, 100.0 mM NaCl, pH 7.4) prior to use. All other chemicals were of analytical grade and used without further purification. Aqueous solutions used throughout were prepared with ultra pure water (>18 MΩ cm) obtained from a Millipore system.

2.2. Apparatus

All electrochemical measurements were performed on a CHI 660B Electrochemical Workstation (Chenhua Instrument Company of Shanghai, China). A conventional three-electrode cell was used with a planar gold (Au) electrode (2 mm in diameter) as the working electrode, a platinum wire as the counter electrode and a saturated calomel electrode (SCE) as the reference electrode.

A definite volume of the GN solution was dropped on the mica surface and air-dried, and then the morphology of GN was characterized by atomic force microscope (AFM, MultiMode, Veeco Instruments Inc., USA) in the tapping-mode at room temperature. The prepared GN powder was further characterized by Raman spectroscopy and the related Raman spectra were recorded on a Renishaw inVia Reflex micro-Raman spectrometer with 633 nm laser excitation.

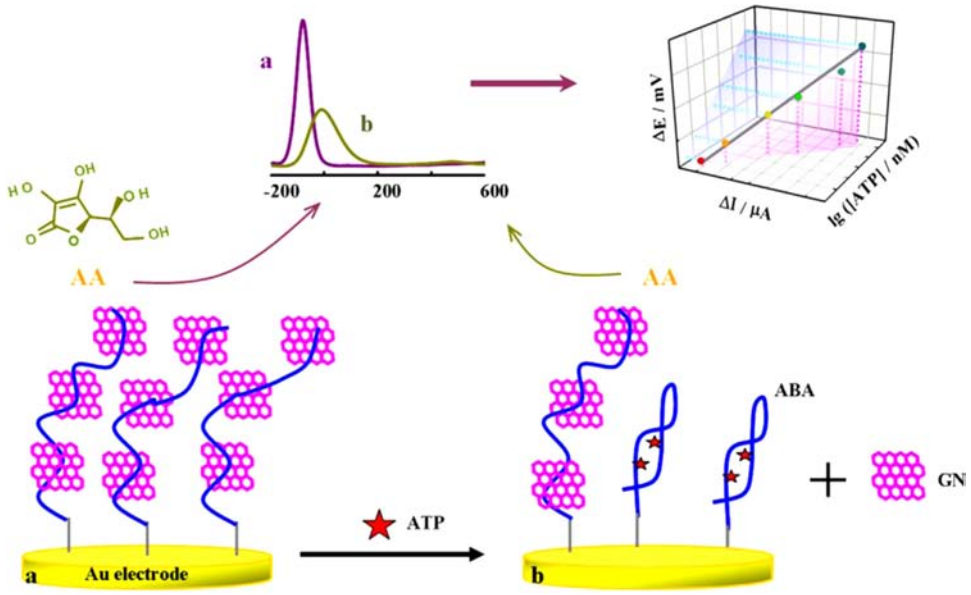

Scheme 1. Schematic illustration for a simple electrochemical ATP aptasensor based on the graphene as nanocatalyst.

2.3. Preparation of the electrochemical aptasensor

Au electrode was firstly polished to mirror-like surface with 0.5 and 0.05-μm alumina slurries, followed by ultrasonication in ultra pure water and ethanol. The electrode was then electrochemically cleaned by immersing it into 0.5 M H_2SO_4 aqueous solution and scanning it with cyclic voltammetry (potential range: −0.3 to 1.5 V, scan rate: 100 mV s^{-1}). After that, the Au electrode was washed thoroughly with copious amount of ultra pure water and dried under nitrogen gas.

20.0 μL of 10.0 μM ABA solution was dropped onto the surface of the clean Au electrode for 16 h at room temperature to obtain the ABA/Au electrode. Then, 10.0 μL of 0.5 mg mL^{-1} GN solution was dropped onto the ABA/Au electrode for 0.5 h to construct the sensing interface (GN/ABA/Au electrode). After each step, electrode was rinsed with washing buffer (10 mM Tris–HCl, pH 7.4) and dried under a stream of nitrogen. To monitor each immobilization step, the electrochemical impedance measurements were performed in 0.1 M KCl aqueous solution with 5.0 mM $[Fe(CN)_6]^{3-/4-}$ as the probe. The impedance spectra were recorded within the frequency range of 100 kHz to 10 mHz at the formal potential of 0.2 V. The amplitude of the alternate voltage was 5 mV. For comparative studies, the GN/NABA/Au electrode was prepared by the same processes.

To demonstrate the electrocatalytic property of GN to AA oxidation, GN/GCE was prepared by casting 5 μL of GN solution onto the surface of the GCE and dried at the room temperature.

2.4. Electrochemical detection of ATP

The aptasensor (GN/ABA/Au electrode) was incubated in 0.5 mL of ATP solution (10.0 mM PBS, 100.0 mM NaCl, pH 7.4) with different concentrations for 0.5 h. After being rinsed with 10.0 mM Tris–HCl (pH 7.4), the electrode was immersed into 1.0 mM AA solution (10.0 mM PBS, 100.0 mM NaCl, pH 7.4). Then, the electrocatalytic oxidation of AA at the GN/ABA/Au electrode was investigated by differential pulse voltammetry (DPV) in the potential range of –0.2 V to 0.6 V (DPV conditions: amplitude, 0.05 V; pulse width, 0.12 s; sampling width, 0.006; pulse period, 0.5 s). Each measurement was repeated at least three times. And the control experiments for GTP, CTP and UTP were carried out at the same conditions.

2.5. Recovery test

For recovery test, fresh urine samples were obtained from healthy volunteers. Each sample was filtered through a 0.2-μm membrane to remove particulate matter. The human-urine samples were diluted separately by a factor of 500 with the buffer solution (10.0 mM Tris–HCl, pH 7.4) and then were equilibrated for 0.5 h at room temperature. The GN/ABA/Au electrodes were firstly incubated in diluted urine samples with different concentrations of ATP for 0.5 h. Then, the electrodes were immersed into 1.0 mM AA solution and the electrocatalytic oxidation signals of AA at the electrodes were investigated by DPV.

3. Results and discussion

3.1. Characterization of GN

GN was prepared by chemical reduction of GO with hydrazine and characterized by AFM. As shown in Fig. 1, the lateral size of GN was 120 nm to 560 nm. The thickness of GN is about 0.97 nm, which matches well with the reported apparent thickness of GN [15,37]. Raman spectrum of GN (Fig. 2) exhibits the presence of D and G bands, and the ratio of the D and G intensities (I_D/I_G) of GN is about 1.14. This indicates that there are significant edge-plane-like defective sites existing on the GN surface and the obtained GN should have good electrocatalytic properties [38].

To demonstrate the electrocatalytic property of the prepared GN to AA oxidation, the electrochemical behaviors of 1.0 mM AA at the bare GCE and GN/GCE were investigated by DPV (Fig. 3). Both the electrodes show the oxidation peaks of AA, which correspond to the oxidation of hydroxy groups to carbonyl groups in furan ring of AA [39]. However, the oxidation potential at GN/GCE is negatively shifted and the peak current increases obviously as compared to bare GCE. Thus, GN in this work can not only accelerate the electron transfer, but also decrease the overpotential of AA oxidation [40]. These demonstrate the obtained GN is a good nanocatalyst for AA electrooxidation.

3.2. Preparation of the aptasensor

In a typical electrochemical impedance spectrum, the semicircle portion observed at higher frequencies corresponds to the charge-transfer limited process. The increase of the diameter of the semicircle reflects the increase of the interfacial charge-transfer resistance (R_{ct}) [41]. As shown in Fig. 4, the bare Au electrode shows a very small semicircle domain, indicating a very fast charge-transfer process [42]. The self-assembly layer of the negatively charged ABA on the Au electrode surface effectively repels the $[Fe(CN)_6]^{3-/4-}$ anions and thus leads to a significantly enhanced charge-transfer resistance (R_{ct}= 15000 Ω, curve b) [43]. GN was then adsorbed onto ABA/Au electrode due to the strong noncovalent binding between GN and nucleobases

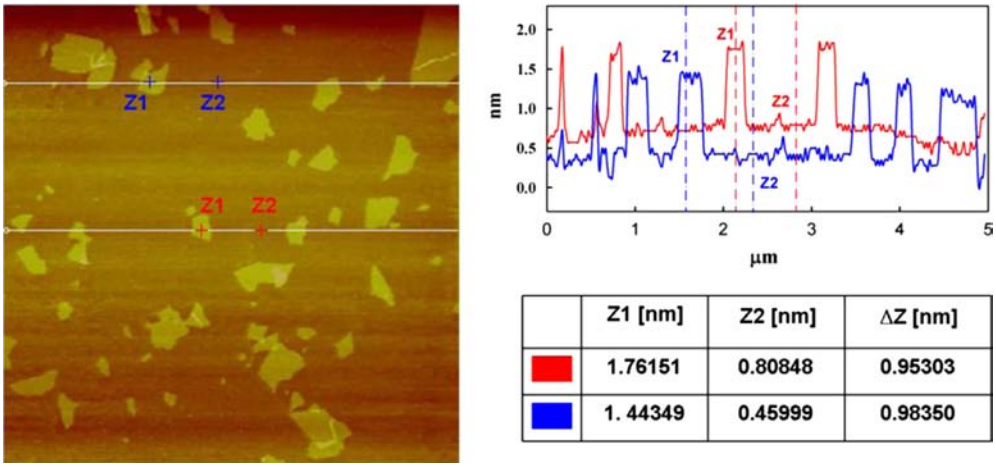

	Z1 [nm]	Z2 [nm]	ΔZ [nm]
	1.76151	0.80848	0.95303
	1. 44349	0.45999	0.98350

Fig. 1. AFM image and the height profiles of GN on mica substrate.

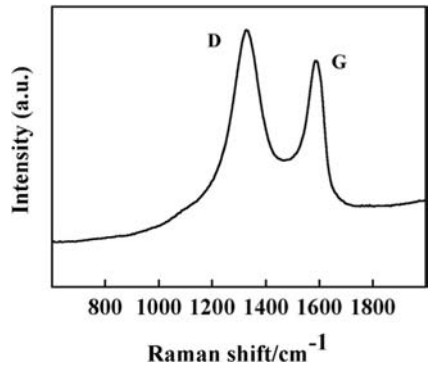

Fig. 2. Raman spectra of GN.

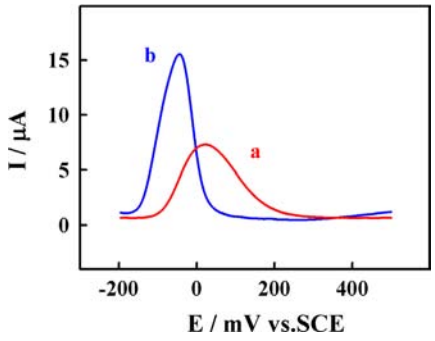

Fig. 3. DPV curves for oxidation of AA at (a) bare GCE and (b) GN/GCE.

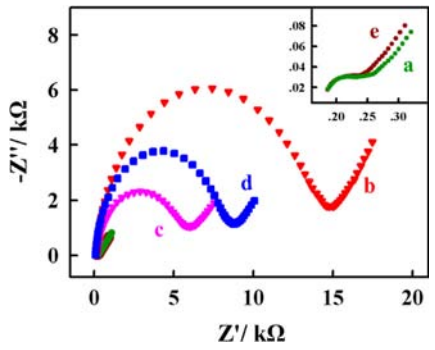

Fig. 4. Electrochemical impedance spectra (Nyquist plots) of the different modified electrodes: (a) bare Au electrode, (b) ABA/Au electrode, (c) GN/ABA/Au electrode, (d) GN/ABA/Au electrode after immersed into 10.0 nM ATP solution for 0.5 h, (e) GN/Au electrode.

[32]. The adsorbed GN with excellent conductivity could highly enhance the electron transfer and an obvious decrease of R_{ct} is observed (R_{ct}=5600 Ω, curve c) [15]. After binding with 10.0 nM ATP, the corresponding R_{ct} increases (R_{ct}=8600 Ω, curve d), because the formation of ATP-ABA complex leads to the release of GN from the sensing interface. However, when 10.0 μL of 0.5 mg mL^{-1} GN solution was directly dropped onto bare Au electrode for 0.5 h without ABA, the resulted GN/Au electrode after washing with 10 mM Tris–HCl (pH 7.4) shows a small semicircle domain (curve e), which is very similar to that of the bare Au electrode. It indicates that few GN can be directly adsorbed onto the bare Au electrode without ABA. All these experimental results demonstrate that the sensing interface (GN/ABA/Au electrode) has been successfully fabricated according to Scheme 1

3.3. Feasibility of the aptasensor

To demonstrate the feasibility of the developed electrochemical aptasensor, DPV responses to the electro-oxidation of 1.0 mM AA at different modified electrodes were investigated. As shown in Fig. 5, an oxidation peak of AA with the peak current of about 4.1 μA and the peak potential of about -37.1 mV can be observed at the bare gold electrode due to its good conductivity (curve a). When ABA is immobilized onto gold electrode, the resulted ABA/Au electrode shows an inconspicuous oxidation signal of AA with low peak current, very positive peak potential and wide peak width (curve b). This should be resulted from the poor electrical conductivity of the ABA/Au electrode and the negatively charged ABA which repels the AA. Because of the superior catalytic property of GN to AA oxidation and its excellent conductivity, the aptasensor after modified with GN (curve c) produces a dramatic increase of the oxidation peak current of AA to about 11.4 μA, accompanied by a substantially negative shift of the peak potential to about −76.0 mV. Then, the GN/ABA/Au electrode was immersed into 10.0 nM ATP solution for 0.5 h (curve d). A part of GN was released from the electrode surface due to the specific ATP-aptamer interaction, leading to the decrease of the loading amount of the GN on the electrode surface. As a result, the oxidation peak current of AA is significantly suppressed to about 4.6 μA, while the related peak potential shifts positively to about -9.0 mV. However, if the GN/ABA/Au electrode is immersed into PBS without ATP for 0.5 h, there are no obvious changes in both peak current and peak potential of AA oxidation (curve e) compared to these at the GN/ABA/Au electrode (curve c). In addition, when the DNA strand which is not the ATP aptamer (NABA) was employed to replace the ABA in the GN/ABA/Au electrode, the signal changes of AA oxidation at the GN/NABA/Au electrode before and after immersed into 10.0 nM ATP solution for 0.5 h are very small (not shown). All of these results suggest that the changes of the oxidation peak current and peak potential of AA at the GN/ABA/Au electrode are owing to the formation of ATP-ABA complex and the release of nanocatalyst GN from the sensing interface.

From Fig. 5, both the electrocatalytic oxidation peak current and peak potential of AA can be correspondingly changed to the addition of ATP. Thus, the resulted aptasensor should have the potential to detect ATP based on the both changes of peak current and peak potential of AA oxidation as the response signals.

3.4. Electrochemical detection of ATP

Fig. 6A shows the DPV responses to the electrocatalytic oxidation of 1.0 mM AA at the GN/ABA/Au electrodes after treated with different concentrations of ATP. It is clearly noted that the oxidation peak current of AA increases and the related peak potential shifts positively with the increase of the ATP concentration.

Figs. 6B and 6C show the relationship between the oxidation peak current (peak potential) of AA and the ATP concentration, and the resulting calibration plots are shown in the inset plots.

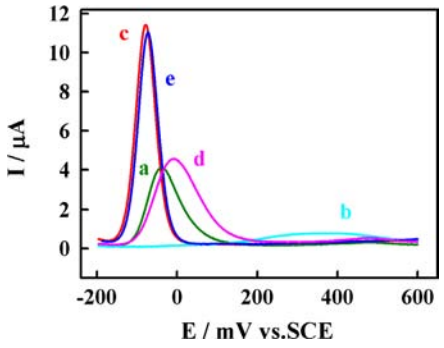

Fig. 5. DPV curves for oxidation of AA at different electrodes: (a) bare Au electrode, (b) ABA/Au electrode, (c) GN/ABA/Au electrode, (d) GN/ABA/Au electrode after incubated in 10.0 nM ATP solution for 0.5 h, (e) GN/ABA/Au electrode after incubated in PBS without ATP for 0.5 h.

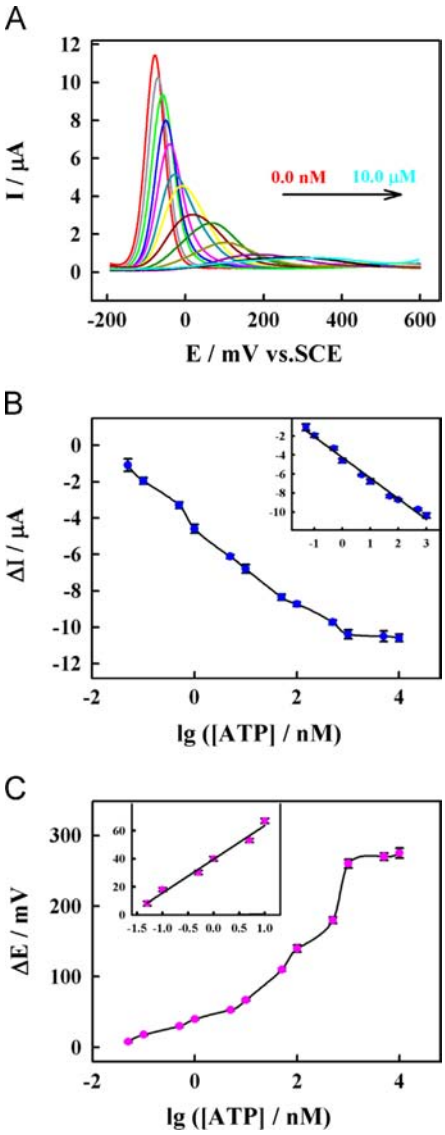

Fig. 6. (A) DPV curves for oxidation of AA at GN/ABA/Au electrodes after incubated with different concentrations of ATP. The concentration of ATP: 0.0, 0.05, 0.1, 0.5, 1.0, 5.0, 10.0, 50.0, 100.0, 500.0 nM and 1.0, 5.0, 10.0 μM. (B) Changes of the AA peak currents against the logarithm of ATP concentration (from 0.05 nM to 10.0 μM). Inset is the linear relationship between ΔI and the logarithm of ATP concentration (from 0.05 nM to 1.0 μM); (C) Changes of the AA peak potentials against the logarithm of ATP concentration (from 0.05 nM to 10.0 μM). Inset is the linear relationship between ΔE and the logarithm of ATP concentration (from 0.05 to 10.0 nM). Error bars represent the standard deviation of three modified electrodes to detect each ATP solutions.

From these figures, the oxidation signals of AA at the GN/ABA/Au electrodes reach the plateau at the high concentration of ATP. Due to the catalytic signal amplification of GN, the obtained aptasensor exhibits excellent analytical performance for sensitive detection of ATP, such as a low detection limit down to 11.7 pM (S/N=3) with a wide linear range of 0.05 nM~1.0 μM (ΔI (μA)= −2.1738 lg([ATP], nM) - 4.2557, R^2=0.9889) while using the change of peak current (ΔI) of AA oxidation as the response signal (the inset plot in Fig. 6B). When using the change of peak potential (ΔE) of AA oxidation as the response signal, a detection limit of 25.0 pM (S/N=3) with a linear range of 0.05 nM~10.0 nM (ΔE (mV)=23.9650 lg([ATP], nM)+39.6071, R^2=0.9856) can be achieved (the inset plot in Fig. 6C). To our best knowledge, these values of the detection limit obtained by our amplified aptasensor, which are based on the superior electrocatalytic property of GN for signal amplification, are much lower than that of other previously reported electrochemical ATP aptasensors (Table 1).

3.5. Selectivity, reproducibility and stability of the aptasensor

In order to investigate the specific response of the aptasensor to ATP, control experiments were performed by incubating the GN/ABA/Au electrodes with several aqueous solutions containing GTP, UTP, CTP (all concentrations are 100.0 nM) and ATP solution (10.0 nM). As illustrated in Fig. 7, the signal changes caused by all other analogues are very small either using ΔI (Fig. 7A) or ΔE (Fig. 7B) of AA oxidation as the response signal, while the ATP sample gives obvious changes of these electrochemical signals. These indicate that the proposed biosensing system has an excellent selectivity for ATP determination.

The reproducibility of the GN/ABA/Au electrode was also investigated. Five modified electrodes were used to detect the same concentration of ATP (10 nM) and the relative standard deviation (RSD) is 5.3% while using ΔI of AA oxidation as the response signal.

Table 1
Comparison of the electrochemical aptasensors for ATP detection[a]

Method	Signal amplifier	Detection limit [M]	Linear range [M]	Reference
DPV	AuNP	1.0×10^{-10}	1.0×10^{-10}~1.0×10^{-7}	[44]
DPV	GO	2.91×10^{-11}	1.0×10^{-10}~5.0×10^{-7}	[33]
SWV			1.0×10^{-8}~1.0×10^{-3}	[45]
DPV	SNP	1.0×10^{-6}		[46]
EIS	GN	1.5×10^{-8}	1.5×10^{-8}~4.0×10^{-3}	[15]
SWV	QD	3.0×10^{-8}	1.0×10^{-7}~1.0×10^{-3}	[47]
SWV	Dual-signaling	1.9×10^{-9}	1.0×10^{-8}~1.0×10^{-4}	[36]
DPV	GN	1.17×10^{-11}	5.0×10^{-11}~1.0×10^{-6}	This work

[a] Abbreviation: Square wave voltammetry (SWV), Electrochemical impedance spectroscopy (EIS), Au nanoparticle (AuNP), Silver nanoparticle (SNP), Quantum dot (QD).

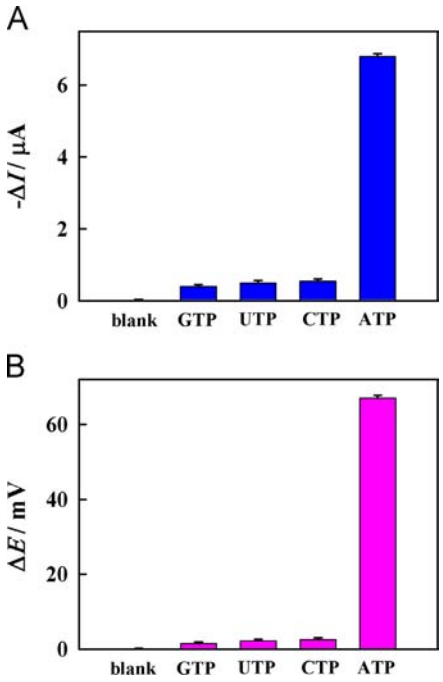

Fig. 7. Selectivity of the biosensor to ATP, CTP, UTP and GTP using ΔI (A) and ΔE (B) as the response signal, respectively. Concentration of ATP is 10.0 nM and the others are 100.0 nM.

Table 2
Recovery assays of ATP in real biological samples.

Sample	Added (nM)	Found (nM)	Recovery (%)
1	10	10.2 ± 0.5	102
2	50	48 ± 3	96
3	100	97 ± 8	97
4	500	526 ± 12	105

Furthermore, the ABA/Au electrode remains bioactive after two-week storage at 4 °C and the response signal of AA at the ABA/Au electrode after modified with GN has no significant change. These demonstrate that the developed electrochemical aptasensor has satisfactory reproducibility and stability.

3.6. Recovery test

The recovery experiments for different ATP concentrations were carried out to evaluate applicability and reliability of the developed aptasensor in complex system. The diluted urine samples were employed as the model of the complex systems in this work. By using ΔI of AA oxidation as the response signal (Table 2), the recoveries for the added ATP with 10.0 nM, 50.0 nM, 100.0 nM, 500.0 nM are 102%, 96%, 97% and 105%, respectively. These results reveal that the recovery of the developed aptasensor is satisfactory and has great practical applications in ATP assay.

4. Conclusions

In summary, based on the superior catalytic property of GN to AA oxidation, a novel label-free electrochemical aptasensor for the amplified detection of ATP has been successfully developed. It shows excellent analytical performance for the electrochemical detection of ATP: based on the change of the oxidation peak current of AA, the ATP detection limit is 11.7 pM (S/N=3) with the linear range of 0.05 nM∼1.0 μM; by using the change of the oxidation peak potential of AA as the response signal, the detection limit is 25.0 pM (S/N=3) with the linear range of 0.05 nM∼10.0 nM. Compared with the previously reported electrochemical assays, our label-free and amplified aptasensor taking GN as nanocatalyst is more simple and sensitive. This is the first time to demonstrate the application of GN as nanocatalyst in an amplified aptasensor. We believe that our new analytical strategy will have very promising applications in other ultrasensitive DNA-based electrochemical sensors.

Acknowledgments

This work was financially supported by NSFC (21275041, 21235002, 21475035, J1210040, J1103312), the Foundation for Innovative Research Groups of NSFC (21221003), Hunan Provincial Innovation Foundation for Postgraduate (CX2013B155), Hunan Provincial Natural Science Foundation of China (12JJ2010), the Specialized Research Fund for the Doctoral Program of Higher Education (20110161110009), and PCSIRT (IRT1238).

References

[1] L.M. Dai, D.W. Chang, J.-B. Baek, W. Lu, Small 8 (2012) 1130–1166.
[2] M. Du, T. Yang, X. Li, K. Jiao, Talanta 88 (2012) 439–444.
[3] Y.X. Fang, E.K. Wang, Chem. Commun. 49 (2013) 9526–9539.
[4] T. Yang, Q. Guan, X.H. Guo, L. Meng, M. Du, K. Jiao, Anal. Chem. 85 (2013) 1358–1366.
[5] Y.X. Guo, Y.J. Guo, C. Dong, Electrochim. Acta 113 (2013) 69–76.
[6] L.-Q. Luo, Z. Zhang, Y.-P. Ding, D.-M. Deng, X.-L. Zhu, Z.-X. Wang, Nanoscale 5 (2013) 5833–5840.
[7] W. Li, P. Wu, H. Zhang, C.X. Cai, Anal. Chem. 84 (2012) 7583–7590.
[8] W. Song, H. Li, H.P. Liu, Z.S. Wu, W.B. Qiang, D.K. Xu, Electrochem. Commun. 31 (2013) 16–19.
[9] A.H. Loo, A. Bonanni, M. Pumera, Nanoscale 5 (2013) 7844–7848.
[10] A.H. Loo, A. Bonanni, M. Pumera, Nanoscale 5 (2013) 4758–4762.
[11] H. Park, S.-J. Hwang, K. Kim, Electrochem. Commun. 24 (2012) 100–103.
[12] G.P. Yan, Y.H. Wang, X.X. He, K.M. Wang, J.Q. Liu, Y.D. Du, Biosens. Bioelectron. 44 (2013) 57–63.
[13] O. Akhavan, E. Ghaderi, R. Rahighi, ACS Nano 6 (2012) 2904–2916.
[14] A. Bonanni, C.K. Chua, G.J. Zhao, Z. Sofer, M. Pumera, ACS Nano 6 (2012) 8546–8551.
[15] L. Wang, M. Xu, L. Han, M. Zhou, C.Z. Zhu, S.J. Dong, Anal. Chem. 84 (2012) 7301–7307.
[16] T. Kuila, S. Bose, P. Khanra, A.K. Mishra, N.H. Kim, J.H. Lee, Biosens. Bioelectron. 26 (2011) 4637–4648.
[17] B. Zheng, J. Wang, F.-B. Wang, X.-H. Xia, Electrochem. Commun. 28 (2013) 24–26.
[18] M.A. Raj, S.A. John, J. Phys. Chem. C 117 (2013) 4326–4335.
[19] H.F. Dong, S. Jin, H.X. Ju, K.H. Hao, L.-P. Xu, H.T. Lu, X.J. Zhang, Anal. Chem. 84 (2012) 8670–8674.
[20] Z.J. Zhang, L. Wu, J.S. Wang, J.S. Ren, X.G. Qu, Chem. Commun. 49 (2013) 9986–9988.
[21] J. Han, Y. Zhuo, Y.Q. Chai, G.F. Gui, M. Zhao, Q. Zhu, R. Yuan, Biosens. Bioelectron. 50 (2013) 161–166.
[22] S.J. Guo, E.K. Wang, Nano Today 6 (2011) 240–264.
[23] R. Polsky, R. Gill, L. Kaganovsky, I. Willner, Anal. Chem. 78 (2006) 2268–2271.
[24] W. Li, P. Wu, H. Zhang, C.X. Cai, Chem. Commun. 48 (2012) 7877–7879.
[25] C.M. Welch, R.G. Compton, Anal. Bioanal. Chem. 384 (2006) 601–619.
[26] C.-C. Kung, P.-Y. Lin, F.J. Buse, Y.H. Xue, X. Yu, L.M. Dai, C.-C. Liu, Biosens. Bioelectron. 52 (2014) 1–7.
[27] C.L.A. Hamula, J.W. Guthrie, H.Q. Zhang, X.-F. Li, X.C. Le, Trends Anal. Chem. 25 (2006) 681–691.
[28] T. Perez-Ruiz, V. Tomas,, J. Martin, Anal. Bioanal. Chem. 377 (2003) 189–194.
[29] J.M. Edward,, M.W. Kevin, J. Am. Chem. Soc. 125 (2003) 12370–12371.
[30] L. Wu, Y. Yang, H.J. Zhang, G.B. Zhu, X.H. Zhang, J.H. Chen, Anal. Chim. Acta 756 (2012) 1–6.
[31] J.X. Wang, X. Zhu, Q.Y. Tu, Q. Guo, C.S. Zarui, J. Momand, X.Z. Sun, F.M. Zhou, Anal. Chem. 80 (2008) 769–774.
[32] L. Wang, X.Y. Qin, S. Liu, Y.L. Luo, A.M. Asiri, A.O. Al-Youbi, X.P. Sun, ChemPlusChem 77 (2012) 19–22.
[33] J.R. Chen, X.X. Jiao, H.Q. Luo, N.B. Li, J. Mater. Chem. B 1 (2013) 861–864.
[34] W.S. Hummers, R.E. Offeman, J. Am. Chem. Soc. 80 (1958) (1339-1339).
[35] D. Li, M.B. Muller, S. Gilje, R.B. Kaner, G.G. Wallace, Nat. Nano 3 (2008) 101–105.
[36] L. Wu, X.H. Zhang, W. Liu, E.H. Xiong, J.H. Chen, Anal. Chem. 85 (2013) 8397–8402.
[37] G. Eda, G. Fanchini, M. Chhowalla, Nat. Nano 3 (2008) 270–274.
[38] A.C. Ferrari, J. Robertson, Phy. Rev. B 61 (2000) 14095–14107.
[39] Z.-H. Sheng, X.-Q. Zheng, J.-Y. Xu, W.-J. Bao, F.-B. Wang, X.-H. Xia, Biosens. Bioelectron. 34 (2012) 125–131.
[40] M. Zhou, Y.M. Zhai, S.J. Dong, Anal. Chem. 81 (2009) 5603–5613.
[41] D.K. Xu, D.W. Xu, X.B. Yu, Z.H. Liu, W. He, Z.Q. Ma, Anal. Chem. 77 (2005) 5107–5113.
[42] Y. Lu, X.C. Li, L.M. Zhang, P. Yu, L. Su, L.Q. Mao, Anal. Chem. 80 (2008) 1883–1890.
[43] C.Y. Deng, J.H. Chen, Z. Nie, M.D. Wang, X.C. Chu, X.L. Chen, X.L. Xiao, C.Y. Lei S.Z. Yao, Anal. Chem. 81 (2009) 739–745.
[44] Y. Du, B.L. Li, F.A. Wang, S.J. Dong, Biosens. Bioelectron. 24 (2009) 1979–1983.
[45] X.L. Zuo, S.P. Song, J. Zhang, D. Pan, L.H. Wang, C.H. Fan, J. Am. Chem. Soc. 129 (2007) 1042–1043.
[46] L. Kashefi-Kheyrabadi, M.A. Mehrgardi, Biosens. Bioelectron. 37 (2012) 94–98.
[47] H.X. Zhang, B.Y. Jiang, Y. Xiang, Y.Y. Zhang, Y.Q. Chai, R. Yuan, Anal. Chim. Acta 688 (2011) 99–103.